6018 J. Med. Chem. 2010, 53, 6018–6027
DOI: 10.1021/jm100231t

Journal of Medicinal Chemistry Article

Strategies for Recognition of Stem−Loop RNA Structures by Synthetic Ligands: Application to the HIV-1 Frameshift Stimulatory Sequence

Prakash B. Palde,[‡] Leslie O. Ofori,[§] Peter C. Gareiss,[‡] Jaclyn Lerea,[†] and Benjamin L. Miller*[,†,‡]

[†]*Department of Dermatology,* [‡]*Department of Biochemistry and Biophysics, and* [§]*Department of Chemistry, University of Rochester, Rochester, New York 14642*

Received February 22, 2010

Production of the Gag-Pol polyprotein in human immunodeficiency virus (HIV) requires a −1 ribosomal frameshift, which is directed by a highly conserved RNA stem−loop. Building on our discovery of a set of disulfide-containing peptides that bind this RNA, we describe medicinal chemistry efforts designed to begin to understand the structure−activity relationships and RNA sequence−selectivity relationships associated with these compounds. Additionally, we have prepared analogues incorporating an olefin or saturated hydrocarbon bioisostere of the disulfide moiety, as a first step toward enhancing biostability. The olefin-containing compounds exhibit affinity comparable to the lead disulfide and, importantly, have no discernible toxicity when incubated with human fibroblasts at concentrations up to 1 mM.

Introduction

The design and synthesis of compounds able to selectively bind specific RNA sequences with high affinity represent a signature challenge in chemistry.[1] Unlike DNA, which to a great extent has been rendered an "open book" for molecular recognition,[2] the problem of sequence-selective RNA recognition remains largely unsolved. In addition to the fundamental importance of this challenge (a subset of the more general challenge of function-oriented synthesis[3]), RNA targets of potential therapeutic value are being discovered at an increasing rate. For example, a notable pathogen against which RNA-targeted therapeutics can potentially have an impact is the human immunodeficiency virus (HIV). The causative agent of AIDS, HIV continues to be a major threat to human life despite intensive ongoing research. While modern antiretroviral drugs have dramatically increased the life spans of those infected with the virus, a number of factors drive the need for new anti-HIV drugs.[4] Key among these include the complexity of current antiretroviral regimens and the emergence of drug resistance.[5−7] Screening and directed design approaches to the development of small molecules interfering with HIV at the RNA level have primarily focused on REV[8] and TAR,[9] and those efforts have yielded a number of important insights into HIV biology, as well as strategies for RNA recognition. Recently, however, another RNA has garnered interest as a potential therapeutic target. This RNA's importance derives from the fact that the structural and enzymatic proteins of HIV are encoded in overlapping *gag* and *pol* open reading frames, respectively.[10] Since *pol* is always translated as a Gag-Pol fusion protein, the ribosome is required to slip one nucleotide backward to produce the desired polyprotein. This −1 frameshift event occurs with a frequency of 5−10%,[11] and disruption of this percentage has been demonstrated to severely decrease viral replication and infectivity.[12]

Two *cis*-acting elements in viral mRNA are responsible for the −1 ribosomal frameshift: a heptameric (UUUUUUA) slippery sequence where the frameshift takes place, and a downstream stimulatory signal.[13] Modification of the stimulatory sequence (either via natural variation or via laboratory mutation) in ways affecting frameshifting efficiency translates to a decrease in viral replication.[14] Thus, targeting this structure with small molecules is a potential strategy for inhibiting viral replication.[15,16] Efforts by several laboratories, including three NMR structural analyses,[17] indicate that the stimulatory RNA in HIV-1 forms a stem−loop structure. This in turn may be divided into an upper stem−loop and lower stem, separated by a purine bulge (Figure 1). It has been hypothesized that frameshift efficiency is dependent on the mechanical stability of the downstream RNA regulatory element, with higher frameshifting rates correlating with a greater force required to unfold the downstream RNA.[18] Recent studies by the Visscher and Fourmy groups suggest that the lower stem and bulge regions of the HIV-1 FSS readily unfold, while unfolding of the upper stem−loop requires more force.[19] Thus, further stabilization (or, alternatively, destabilization) of the upper stem−loop may alter frameshift efficiency, suggesting that this sequence may constitute a useful target for drug discovery. We have previously reported the discovery of a compound (**1**) able to selectively bind the HIV-1 frameshift-stimulating RNA upper stem−loop (hereafter abbreviated "HIV-1 FSS"[a]).[20] Compound **1** was identified via the synthesis and *in situ* screening of an 11325 member resin-bound dynamic combinatorial library (RBDCL) designed based on a core structure inspired by nucleic acid binding, bisintercalating natural products.[21] This molecule binds the HIV-1 FSS with a dissociation constant (K_D) of 4.1 ± 2.4 μM as measured by surface plasmon resonance (SPR) and

*To whom correspondence should be addressed. E-mail: Benjamin_Miller@urmc.rochester.edu. Phone: 585-275-9805. Fax: 585-273-1346.

[a] Abbreviations: HIV-1 FSS, frameshift-stimulating RNA sequence of HIV-1; SPR, surface plasmon resonance; RBDCC, resin-bound dynamic combinatorial chemistry; RBDCL, resin-bound dynamic combinatorial library; MTT, 3-(4,5-dimethylthiazol-2-yl)-2,5-diphenyltetrazolium bromide.

 Published on Web 07/30/2010

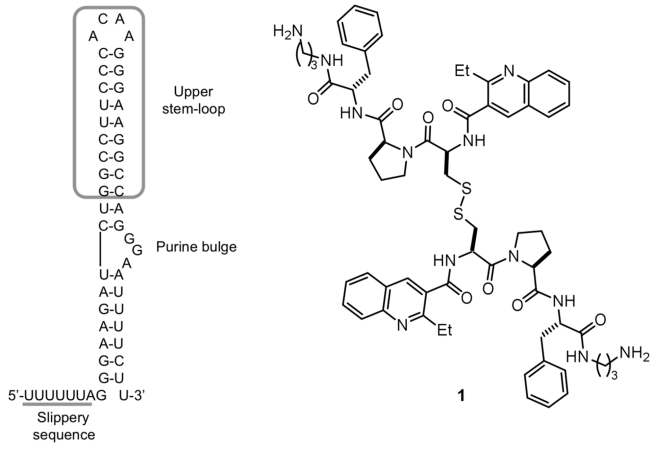

Figure 1. (Left) Secondary structure of the HIV-1 frameshift-inducing RNA stem−loop. The sequence shown is that of the HIV group M subtype D.[25] The upper stem−loop sequence (or "HIV-1 FSS") used as the primary target for RBDCC screening and for the experiments described herein is boxed. The slippery sequence where the −1 frameshift occurs is underlined. (Right) Lead molecule **1**, previously identified via RBDCC.

serves as an important lead for the development of high-affinity ligands for the HIV-1 FSS. Other recent reports of compounds targeting frameshifting in HIV include a description by Butcher and Tor of the interaction of guanidinoneomycin with the HIV-1 FSS upper stem−loop[22] and a recent report of several molecules targeting the bulge region.[23] This latter study suggests that the question of the "best" region of the FSS to target should not yet be regarded as settled. Heveker and colleagues have described peptides able to interfere with frameshifting in a two-reporter bacterial system, but it is uncertain whether this interference involves a direct interaction with the FSS.[24]

This paper details our efforts to expand our understanding of the structural factors governing recognition of the HIV-1 FSS by **1**. We approached the problem via solution-phase binding analysis and by the directed synthesis of several analogues of **1** to explore structure−activity relationships with a particular focus on modifications to the quinoline heterocycle. As part of the structure−activity analysis, we also report the first steps toward enhancing the biostability of **1**, via the synthesis and binding analysis of analogues of **1** incorporating hydrocarbon replacements (bioisosteres) for the disulfide.

Analysis of the Binding Selectivity of 1. Previously reported SPR measurements on **1** were conducted with the compound tethered to the SPR chip via one of its amino groups and involved a relatively limited set of RNA sequences. As a first step toward increasing our understanding of the interaction of **1** and related compounds with the HIV-1 FSS, we carried out a series of solution-phase fluorescence titration measurements. In these experiments, the fluorescence of 5′-Cy3-labeled RNA was monitored as a function of added compound.[26,27]

The RNA and DNA sequences employed and results of titrations (alongside previously reported SPR values, where available) are shown in Table 1; selected titration data and associated curve fits are shown in Figure 2. All data were fit to a 1:1 binding model incorporating ligand depletion. Binding to the HIV-1 FSS derived from HIV group M subtype D (entry 1) was found to be 0.35 ± 0.11 μM in solution, roughly an order of magnitude tighter than the binding constant obtained previously by SPR. This is not altogether surprising, as immobilization of **1** on the SPR chip reduces both the degrees of freedom available to the compound and its overall charge. The measured binding affinity of **1** for the HIV-1 FSS did not change in the presence of an excess of unrelated competing RNAs (either yeast tRNA, entry 2, or total yeast RNA, entry 3), although the total change in fluorescence decreased. To confirm that this reduction in the total change in fluorescence reflected a nonspecific interaction between the Cy3-labeled HIV-1 FSS and competitor RNAs rather than off-target binding by compound **1**, we titrated an identical solution of yeast tRNA into Cy3-labeled HIV-1 FSS. Consistent with our hypothesis, the dilution-corrected Cy3 fluorescence decreased in a manner dependent on the concentration of tRNA (Supporting Information, p S32). Use of excess yeast tRNA as a measure of selectivity was pioneered by Tor and colleagues;[28] following Tor's terminology, where "specificity" is defined as the ratio of the K_D to the sequence of interest over the K_D observed in the presence of a large excess of competitor RNAs, our results suggest a specificity ratio of approximately 1. As expected, the measured binding constant could be altered by addition of unlabeled (competing) HIV-1 FSS (entry 4).

Single mutation (entry 5) or complete sequence flipping (entry 6) of the stem did not produce an experimentally significant change in the binding constant. In contrast, the introduction of single (entry 7) or multiple (entry 8) mutations into the loop region caused a 2-fold and 4-fold reduction in the binding, respectively. No saturable binding was observed to a DNA homologue of the HIV-1 FSS (entry 9) or to unrelated RNA hairpins (entries 10 and 11; note that these sequences have been examined in previous studies in our laboratory[29] and are known to be folded under the conditions of the titrations). Taken together, these results confirm that compound **1** binds the target HIV-1 FSS with high affinity and good selectivity. Alterations to the tetraloop had the greatest impact on binding.

Structure−Activity Relationships of the 2-Ethylquinoline-3-carboxamide Moiety. With a more detailed understanding of the solution-phase binding selectivity of **1** in hand, we next turned toward modifications of the compound itself in order to examine the structural features governing binding. On the basis of prior reports of the ability of quinolines to act as general (non-sequence-selective) RNA intercalators,[1b] one would hypothesize intercalation as the primary function of the 2-ethylquinoline-3-carboxamide moieties of **1**. To test that hypothesis, compounds **2**−**7** were synthesized on solid-phase resin beads using methods previously described for the synthesis of **1**. Binding constants were measured by fluorescence titration (Table 2). Changing the 2-ethyl group to methyl (**2**) or proton (**3**) yielded experimentally insignificant (**2**) or only modest (**3**) reduction in affinity for the HIV-1 FSS. This is consistent with molecular mechanics calculations indicating that there is little difference in the conformational landscape of these three compounds. Decreasing the available π-surface, exemplified in the 2-methyl-3-carboxypyridine compound (**4**) and uncapped peptide (**5**), completely ablated binding. This stark difference in affinity between **1** and **5** was confirmed by a filter-binding assay (Supporting Information, Figure S7). The introduction of a dioxolane ring (**6**) resulted in a compound with roughly 4-fold lower affinity than **1**, while replacement of the quinoline with an anthraquinone yielded a molecule (**7**) with affinity equivalent to **1**.

Table 1. Binding Constants (K_D, μM) for **1** and Selected Oligonucleotides[a]

Entry	Sequence	SPR	Solution
1	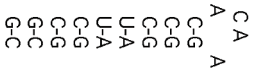	4.1±2.4	0.35 ± 0.11
2	As entry 1, + 40x total yeast tRNA	ND	0.20 ± 0.03
3	As entry 1, + 20x total yeast RNA	ND	0.57
4	As entry 1, + 4x unlabeled HIV-1 FSS	ND	0.65 ± 0.13
5	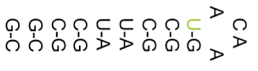	ND	0.45 ± 0.04
6		ND	0.33 ± 0.12
7	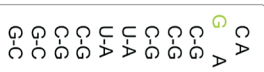	ND	0.76 ± 0.06
8		>90	1.10 ± 0.1
9	 (DNA homolog)	No binding	No binding
10		No binding	No binding
11	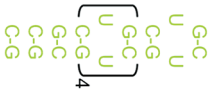	ND	>40

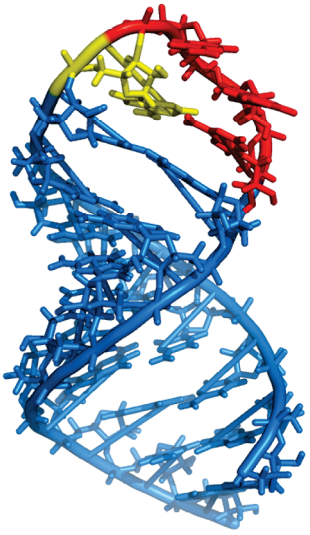

[a] "Solution" measurements were carried out by titrating unlabeled compound into Cy3-labeled RNA and measuring changes in the fluorescence spectrum, while SPR measurements were performed by immobilizing the compound on the sensor chip and flowing increasing concentrations of unlabeled RNA. ND = not determined. Right: Butcher et al. NMR structure of the HIV-1 FSS RNA (PDB code 1PJY)[17a] color-coded by binding constant change in altered sequences (blue = least; red = most).

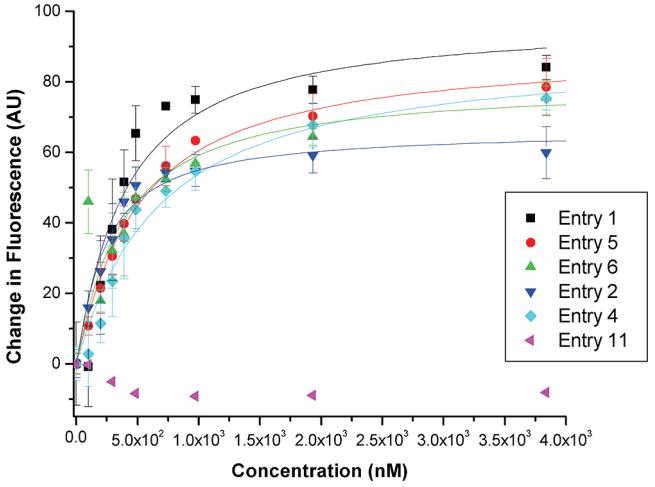

Figure 2. Selected fluorescence titration data (dilution-corrected fluorescence change as a function of ligand concentration) and curve fits for the experiments summarized in Table 1.

Observation that 2-methylpyridine derivative **4** is unable to bind supports an intercalative binding mechanism for **1**, as it is well-known (at least in a DNA-binding context) that pyridines have insufficient π-surface area to support intercalation. As discussed below, the $(Cys\text{-}Pro\text{-}Phe)_2$ peptide is not a passive player in binding, however, despite the lack of RNA-binding affinity displayed by **4** and **5**. Further efforts are underway to explore the ability of other heterocycles with larger π-surface area to enhance affinity.

Replacement of the Disulfide with Nonlabile Bioisosteres. The ability of the disulfide to undergo exchange with other thiols in solution[30] was a critically important design feature of the RBDCL used to identify **1**. However, its susceptibility to reduction or exchange in a biological environment would present an obvious obstacle to investigation of this class of molecules in a cellular context. Reduction is particularly a concern in the cytosol, where the ratio of reduced:oxidized glutathione (GSH:GSSG) ranges from 30:1 to 100:1.[31] Previous work has shown that in most "biologically active" peptides the disulfide linkage serves only a structural role and replacing it with thioether ($-S-CH_2-$) or all carbon (olefin, $-CH_2-CH_2-$) bioisosteres generally enhances biostability of the molecule without affecting its function.[32] A particularly striking example of the interchangeability of disulfide and olefin linkages was reported in 2000 by Nicolaou and co-workers, who found similar selectivities in the receptor-accelerated synthesis of disulfide- and olefin-linked

Table 2. Binding Constants (K_D) for Heterocycle Analogues of **1** Binding to the HIV-1 FSS RNA, As Measured by Fluorescence Titration[a]

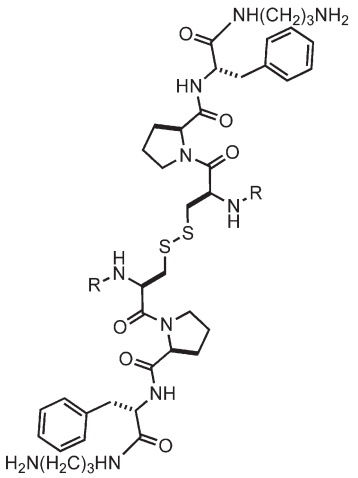

Compound	R	MW	K_D (μM)
1	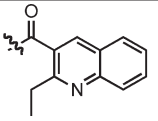	1206	0.35 ± 0.11
2	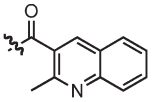	1178	0.43 ± 0.05
3	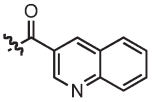	1150	0.65 ± 0.04
4	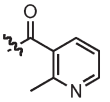	1078	No Binding
5	H	840	No Binding
6	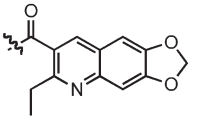	1295	1.42 ± 0.17
7	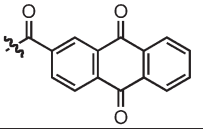	1308	0.23 ± 0.03

[a] All values are an average ± standard deviation of three replicate titrations. Compounds **1**−**7** all likely carry a charge of +2.

vancomycin dimers.[33] Saturated hydrocarbon analogues of disulfides have also been reported, for example, in the enkaphalins.[32d] Therefore, in order to build toward compounds suitable for cellular studies, we next synthesized dicarba (olefin and hydrocarbon) analogues of compound **1**.

Ruthenium-catalyzed olefin metathesis is an attractive and powerful tool for the formation of carbon−carbon double bonds.[34] Grubbs' catalysts (first and second generation) have been previously used in the synthesis of cyclic peptides via ring-closing metathesis.[32,35] Likewise, olefin cross-metathesis of amino acid derivatives[36] and more complex peptides is well established. Therefore, to substitute for the cysteine amino acid in **1**, the olefin was introduced in the form of L-allylglycine.[37] Following preparation of the metathesis precursor peptide **8**, initial efforts focused on carrying out olefin self-metathesis of this compound in solution. However, we were unable to remove all traces of catalyst from the product olefin-containing peptide despite the application of various catalyst removal strategies.[38] To avoid this issue, we turned to the use of on-bead cross-metathesis between resin-bound and solution-phase **8**. As shown in Scheme 1, cleavage of the resin-bound adduct following cross-metathesis gave a mixture of geometrical isomers (**9** and **10**) in a 2:3 ratio and 64% yield. The mixture was then separated by preparative HPLC to give the purified *E* and *Z* isomers. Preparation of the saturated analogue **11** was accomplished by on-bead hydrogenation of metathesis adduct (Wilkinson's catalyst; 40 psi H_2), followed by TFA-mediated cleavage.

As measured by fluorescence titration, both **9** and **10** bound to the HIV-1 FSS with an affinity comparable to that of compound **1**. Thus, bioisosteric replacement of the disulfide linkage in **1** with an olefin does not interfere with RNA recognition (Table 3). Olefin isomers **9** and **10** show only a 2-fold difference in their binding affinity, suggesting that the linker is sufficiently flexible to access a favorable conformation for binding regardless of olefin geometry. The 4-fold decreased affinity of the saturated analogue (**11**) relative to **1** may be either a reflection of the increased flexibility of the compound relative to the olefin bioisostere or potentially a result of its increased hydrophobicity. As with compound **1**, the binding affinity of dicarba analogues to the stem−loop was unchanged in the presence of excess yeast tRNA, evidence of selectivity for binding to the HIV-1 RNA stem−loop. Interestingly, monomeric compound **8** also bound to the HIV-1 RNA stem−loop with similar affinity to that of both the parent compound (**1**) and analogues **9** and **10**, but binding was completely ablated by the presence of excess yeast tRNA. This is similar to the behavior shown by 2-ethylquinoline-3-carboxylic acid, which binds RNA nonspecifically. Thus, both the full-length peptide and quinoline are required for selective binding to the HIV-1 FSS.

Study of Binding Kinetics Using SPR. While the equilibrium dissociation constant (K_D) is obviously an important measure of ligand quality *in vitro*, kinetic parameters (and, in particular, the dissociation rate k_{off}) have been proposed as more effective predictors of *in vivo* selectivity.[39] Slower values for k_{off} mean longer target-bound residence times[40] and higher target selectivity. In contrast, increases in k_{off} have been correlated with decreases in inhibitor activity.[41] Therefore, to assess the kinetics of binding by dicarba analogues, we turned to surface plasmon resonance.

For binding studies using SPR, biotinylated HIV-1 FSS RNA was immobilized on a Biacore CM5 SPR sensor chip coated with streptavidin. Compounds **1** and **9**−**11** were then flowed over the HIV-1 FSS RNA functionalized SPR chips in the running buffer (1× PBS buffer equipped with 5 mM $MgCl_2$ and 0.005% Tween-20). Representative sensorgrams

Scheme 1. Synthesis of Olefin and Saturated Hydrocarbon Analogues of **1**

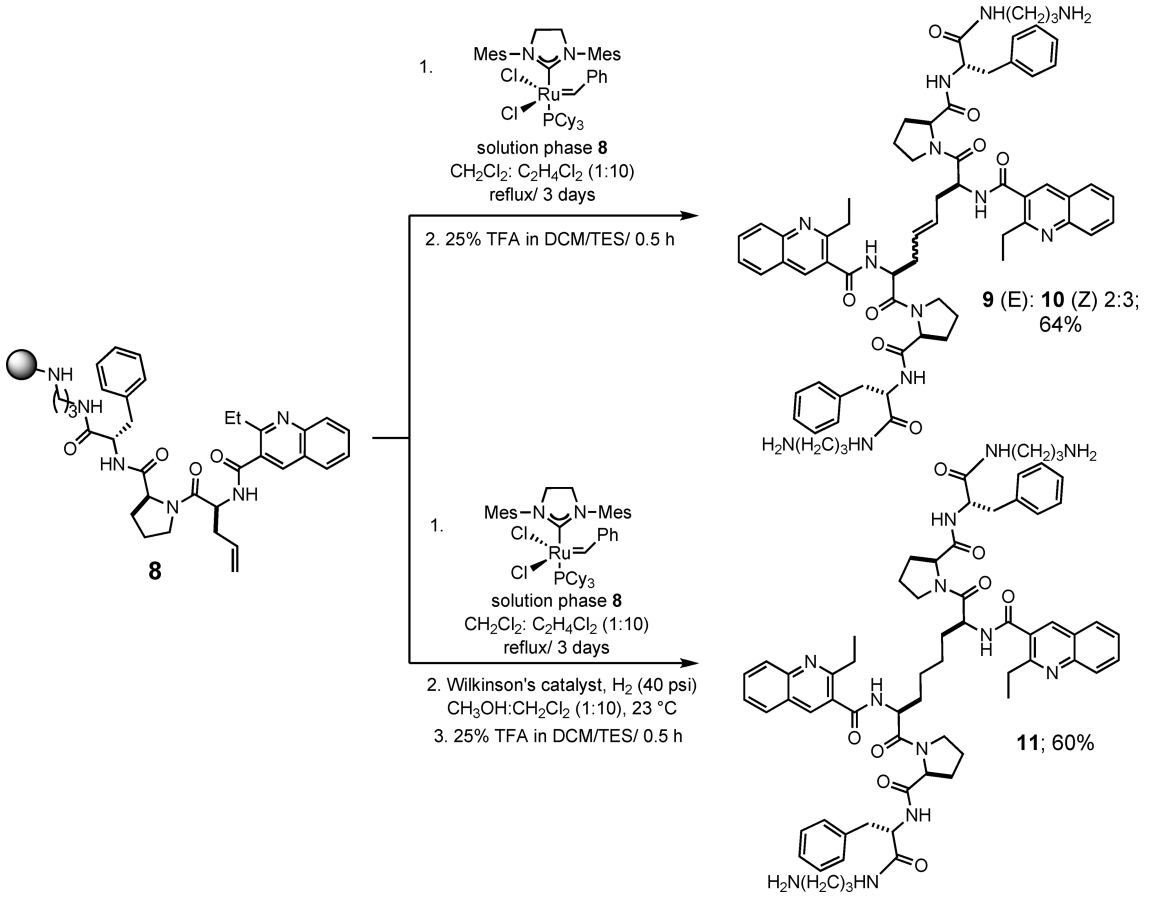

Table 3. Binding Affinity of Dicarba Analogues to the HIV-1 FSS RNA (4×10^{-7} M) in Comparison to **1** As Measured by Fluorescence Titrations in 1× PBS Buffer (pH 7.2) at 25 °C[a]

compound	MW	charge	binding affinity (K_D) (μM)	binding affinity (K_D) in the presence of 20× yeast tRNA (μM)
1		2	0.35 ± 0.11	0.20 ± 0.03
2-ethylquinoline-3-carboxylic acid	201	−1	0.29 ± 0.03	no binding
8	598	1	0.47 ± 0.04	no binding
9	1168	2	0.33 ± 0.02	0.39 ± 0.02
10	1168	2	0.18 ± 0.02	0.26 ± 0.04
11	1170	2	1.27 ± 0.11	1.41 ± 0.20

[a] The reported K_D values are an average of two separate titration experiments in each case.

Table 4. Evaluation of Binding Kinetics Using SPR[a]

compound	dissociation rate (k_{off}) (s^{-1})	association rate (k_{on}) (M^{-1} s^{-1})	dissociation constant (K_D) (μM)	chi^2
1	1.41×10^{-2}	1.79×10^{3}	7.88	1.07
9	1.28×10^{-2}	1.15×10^{3}	11.20	1.85
10	7.5×10^{-3}	1.62×10^{3}	4.66	2.73
11	1.3×10^{-2}	1.05×10^{3}	12.30	1.09
neomycin	ND	ND	2.6	0.18

[a] The kinetic parameters k_{on} and k_{off} were obtained from a 1:1 global fit to six sensorgrams generated by injecting different concentrations of each ligand. The dissociation constant (K_D) for neomycin was obtained from a steady-state analysis of seven sensorgrams; obtaining kinetic constants for this compound was not possible.

are provided in Supporting Information, while kinetic and equilibrium binding constants are summarized in Table 4. The binding constant ($K_D = 7.88\,\mu$M) obtained for **1** (Table 4) in this experimental setup (where HIV-1 FSS RNA is immobilized onto the chip, or the reverse of our previously reported method) is in conformity with the binding constant ($K_D = 4.1 \pm 2.40\,\mu$M) measured with the earlier experiments. It is interesting to note that immobilization of either binding partner for SPR appears to cause an order-of-magnitude loss in the affinity of these compounds relative to solution-phase measurements. Likewise, measured dissociation constants for **9**−**11** were at least 10-fold weaker in this format than in the fully solution phase measurements.

The kinetic data obtained from SPR studies (Table 4) show that the k_{off} of compounds **1** and **9**−**11** lie in the range of 10^{-2} to 10^{-3} s^{-1}, corresponding to a dissociative half-life ($t_{1/2} = 0.693/k_{off}$) of 50−90 s. Dissociative half-life is a parameter that determines the residence time of a ligand at the

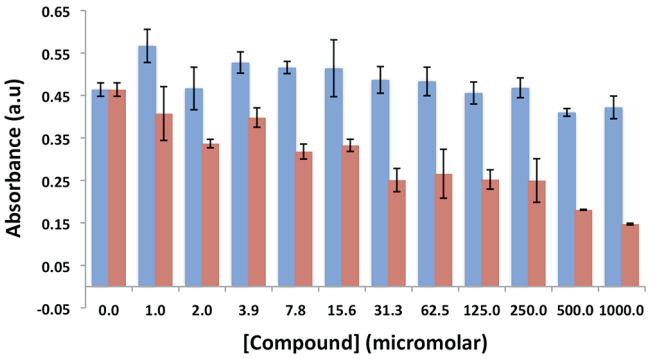

Figure 3. MTT assay for compound **10** (blue) vs mitomycin C (red). Results suggest that compound **10** is nontoxic to human fibroblasts at concentrations up to 1.0 mM.

target site, which in turn governs target selectivity. Indeed, it has been hypothesized that the poor selectivity shown by some aminoglycosides is due at least in part to their relatively high k_{off} (significant amount of dissociation in 30 s).[42] To test this in the context of the HIV-1 FSS sequence, we examined the binding of neomycin by SPR. While steady-state methods could be used to derive a binding constant (2.6 μM), both k_{on} and k_{off} were too rapid to determine accurately from the data (Supporting Information, Figure S13). This is consistent with the hypothesized relationship between the off rate and sequence selectivity, as unlike our compounds neomycin is known to bind with similar affinity to a diverse range of RNAs.[1] Hence, these data support the assertion that compounds of the structural class defined by **1**, **9**, **10**, and **11** are promising candidates for further development as selective RNA-binding ligands.

While the analyses described thus far suggest compounds **9**−**11** possess significant selectivity for target RNA sequences, a more stringent test is to examine their compatibility with cells, since a lack of selectivity in RNA-binding ability can manifest as toxicity.[43] We therefore determined the tolerance of human fibroblasts to compound **10** using the widely employed MTT assay,[44] which serves as a reporter for mitochondrial activity. We were gratified to observe that compound **10** caused no statistically significant change in cell viability at concentrations up to 1.0 mM. In contrast, mitomycin C, a DNA cross-linking agent widely used in chemotherapy, caused significant cell death at all concentrations tested (Figure 3).

In conclusion, we have employed directed analogue synthesis to improve our understanding of the interaction of RBDCC-derived compounds with the HIV-1 FSS RNA, a critical regulatory element of HIV replication. The picture that emerges based on the data obtained to date is that the 2-ethyl-3-carboxyquinoline moieties of **1** and dicarba analogues **9**−**11** are the primary source of *affinity*, most likely via intercalation, while *selectivity* of binding resides in the peptide (Figure 4). Replacement of the disulfide moiety with an olefin bioisostere does not diminish activity, a discovery that is an important first step toward the production of compounds suitable for cellular assays of frameshifting. Finally, compounds are nontoxic to cells at relevant concentrations. Neither compound **1** nor analogues **9**−**11** are sufficiently conformationally rigid to permit generation of meaningful hypotheses with regard to their RNA-bound conformation in the absence of experimental data; thus, X-ray or NMR structural analysis will be an important next step toward

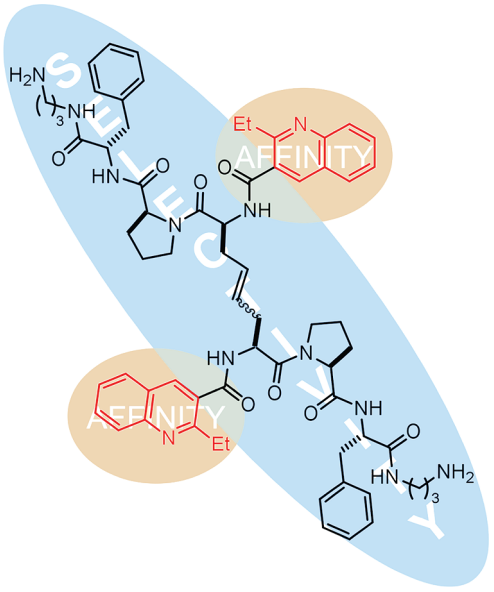

Figure 4. Schematic of binding results for analogues described herein: selective, high-affinity binding to the HIV-1 FSS requires both peptide and heterocyclic portions of lead compounds. Affinity is largely determined by the presence of the quinoline moiety, while selectivity derives from the peptide. Binding appears insensitive to olefin geometry.

understanding the behavior of these compounds. Efforts are underway to employ this newfound understanding in the design and synthesis of new compounds with further improved affinity, selectivity, and biostability. In particular, as substantial portions of **9** and **10** are still peptidic, conversion to peptidomimetic structures is a primary current focus. It is also not yet clear whether the full peptide is required for selectivity, and therefore deletion studies will be important to test that question. Completion of these experiments will set the stage for *in vitro* studies designed to test the ability of such RNA-binding compounds to interfere with frameshifting in HIV.

Experimental Section

Materials and General Methods. Commercially available reagents were obtained from Aldrich Chemical Co. (St. Louis, MO), Fluka Chemical Corp. (Milwaukee, WI), and TCI America (Portland, OR) and used as received unless otherwise noted. Water used for reactions and aqueous workup was doubly distilled. Reagent grade solvents were used for all nonaqueous extractions. Reactions were monitored by analytical thin-layer chromatography using EM silica gel 60 F-254 precoated glass plates (0.25 mm). Compounds were visualized on the TLC plates with a UV lamp (λ = 254 nm) and staining with I_2/SiO_2. Synthesized compounds were purified using flash chromatography on EM silica gel 60 (230−400) mesh or, alternatively, via preparative reverse-phase HPLC.

Analysis. ^{1}H NMR spectra were recorded at 25 °C on either a Bruker Avance 400 (400 MHz) or a Bruker Avance 500 (500 MHz) instrument. Chemical shifts (δ) are reported in parts per million (ppm) downfield from tetramethylsilane and referenced to the residual protium signal in the NMR solvent ($CDCl_3$, δ = 7.26). Data are reported as follows: chemical shift, multiplicity (s = singlet, d = doublet, t = triplet, m = multiplet), integration, and coupling constant (J) in Hertz (Hz). ^{13}C NMR spectra were recorded at 25 °C on a Bruker Avance 400 (100 MHz) or Bruker Avance 500 (125 MHz). Chemical shifts (δ) are reported in parts per million (ppm) downfield from tetramethylsilane and referenced to carbon resonances in the NMR solvent.

High-resolution mass spectra (HRMS) were acquired at the University of Buffalo mass spectrometry facility, Buffalo, NY, or at the mass spectrometry facility of the University of California, Riverside.

Binding Analysis. Fluorescence titrations were performed on a Cary Eclipse fluorescence spectrophotometer using a 10 mm path-length semimicro quartz fluorescence cell with 400 μL sample holding capacity. The 5′-Cy3-labeled HIV-1 FSS RNA was purchased from Integrated DNA Technologies, Inc. Autoclaved 1× phosphate-buffered saline (PBS) (4.3 mM Na_2HPO_4, 1.47 mM KH_2PO_4, 137 mM NaCl, 2.7 mM KCl; pH = 7.2) was used as a buffer to dissolve the RNA and the compounds to be tested. A solution of HIV-1 FSS RNA in 1× PBS buffer (400 μL, 400 or 500 nM) was heated to 65 °C for 4 min, and 2 μL of a $MgCl_2$ solution (1 M) was added to it. The solution was then allowed to cool slowly to room temperature in the presence of $MgCl_2$ in order to ensure that the RNA assumes its secondary stem−loop structure. This solution of 5′-Cy3-labeled HIV-1 FSS RNA was taken in the cell and excited with a wavelength of 550 nm and a 2.5 nm slit width. The emission spectrum was collected from 555 to 600 nm wavelength range at a PMT voltage of 715 V and a 5 nm slit width. The compound in 1× PBS buffer was added to the cell in either 2 or 4 μL increments from the stock solution (either 20, 50, or 200 μM) leading to a concentration range starting from 100 nM to 10 μM. After each addition, the solution was allowed to equilibrate for a minimum of 10 min, and fluorescence emission spectra were taken. Equilibrium was determined to be established after obtaining three similar fluorescence spectra taken at 1 min intervals. The decrease in fluorescence of 5′-Cy3-labeled HIV-1 FSS RNA was then noted at 564.1 nm for each added concentration of the compound. The fluorescence units (FU) were then dilution corrected, and the FU after each addition was subtracted from the FU at zero compound concentration to give ΔFU. This ΔFU was plotted against compound concentration using Origin 7 (OriginLab Corp.). The data were fit to a one-site binding model accounting for ligand depletion.[45] In this analysis, the free ligand concentration term is substituted with total ligand concentration minus the bound ligand concentration ($L_T - B$) as

$$B = \frac{R_T(L_T - B)}{K_D + (L_T - B)}$$

Solving the equation for B (real solution for the quadratic equation)

$$B = \frac{(L_T + K_D + R_T) - \sqrt{(-L_T - K_D - R_T)^2 - 4L_T R_T}}{2}$$

where B = bound ligand:receptor complex concentration, L_T = total ligand concentration, K_D = dissociation constant, and R_T = total receptor concentration.

Titrations were carried out with each compound at least two times. Buffer control titrations were performed by titrating similar amounts of PBS, pH 7.2, into the Cy-3 RNA and confirmed a concentration-dependent linear fluorescence change matching what is theoretically expected. For the competition experiments with yeast total tRNA, the competing RNA was added to the 5′-Cy3-labeled HIV-1 FSS RNA at a concentration of 8 or 16 μM. This mixture of RNA was then titrated with the compounds in a similar manner described above. Titrations into other labeled sequences (entries 5 through 11, Table 1) were carried out analogously to the procedure employed for the HIV-1 FSS RNA. Surface plasmon resonance (SPR) experiments were conducted using a Biacore-X instrument (GE Healthcare); procedures are described in the main text and in greater detail in the Supporting Information.

Synthesis of Analogues 2−7. Compounds **2**−**7** were synthesized on resin using methods previously described for compound **1**. Following completion of the synthesis, compounds were cleaved from resin, ether precipitated, and purified by reverse-phase preparative HPLC using a water−acetonitrile gradient with 0.1% TFA. Purified compounds were verified as being >95% purity by analytical HPLC.

Compound 2. FTIR (neat): 3065.52, 3018.87, 2953.30, 2920.99, 2915.69, 1664.45, 1643.24, 1634.56, 1538.12, 1433.38, 1312.95, 1296.08, 1241.50, 1198.68, 1173.60, 1125.87, 1021.72, 952.29 cm^{-1}. ^1H NMR (400 MHz, CD_3OD): δ 8.6 (s, 1H), 8.58 (s, 1H), 8.06 (d, 1H, J = 8.3), 8.03−7.83 (m, 6H), 7.71−7.61 (t, 1H, J = 7.34, J = 7.83), 7.30−7.7.12 (m, 10H), 7.09 (d, 4H, J = 6.85), 5.33 (q, 1H, J = 4.88), 4.5−4.3 (m, 4H), 4.01−3.91 (m, 1H), 3.91−3.78 (m, 2H), 3.59−3.50 (m, 1H), 3.5 (dd, 1, J = 9.23, J = 4.88), 3.40−3.30 (m, 1H), 3.27−2.96 (m, 2H), 2.90−2.70 (m, 10H), 2.71−2.65 (t, 2H, J = 1.95, J = 2.93), 2.66−2.56 (s, 3H), 2.22−2.04 (m, 4H), 2.05−1.91 (m, 4H), 1.92−1.79 (m, 4H), 1.80−1.67 (m, 6H), 1.66−1.46 (m, 4H). ^{13}C NMR (100 MHz, CD_3OD): δ 172.5, 169.6, 167.7, 161.45, 161.1, 156.4, 143.9, 136.9, 132.6, 129, 128.8, 128.2, 127.8, 127.7, 126.5, 125.9, 124.3, 60.7, 56.6, 55.1, 51.1, 39, 36.9, 36.6, 35.5, 28.9, 27.1, 24.5, 20.9. HRMS m/z calculated for $C_{62}H_{75}N_{12}O_8S_2$ $[M + H]^+$: 1179.5267; found: 1179.5299.

Compound 3. FTIR (neat): 3068.12, 2960.53, 2940.76, 2450.23, 2270.34, 1651.43, 1634.08, 1538.12, 1435.90, 1199.16, 1127.32 cm^{-1}. ^1H NMR (400 MHz, CD_3OD): δ 9.08 (s, 1H), 8.68 (d, J = 18.2, 1H), 8.06−7.75 (m, 6H), 7.62 (dd, J = 17.0, J = 10.1, 2H), 7.32−7.07 (m, 10H), 5.35−5.21 (m, 2H), 4.53−4.32 (m, 3H), 4.23 (d, J = 8.4, 1H), 4.07 − 3.91 (m, 2H), 3.80 (s, 2H), 3.55−2.89 (m, 22H), 2.76 (dd, J = 14.5, J = 7.2, 4H), 2.10 (dd, J = 19.8, J = 8.1, 2H), 2.00−1.63 (m, 9H), 1.67−1.35 (m, 2H). ^{13}C NMR (100 MHz, CD_3OD): δ 172.6, 170.0, 161.2, 147.7, 137.2, 136.8, 132.0, 128.8, 126.9, 126.5, 60.7, 59.3, 55.1, 54.1, 50.1, 39.1, 39.8, 36.5, 35.4, 28.8, 27.1, 25.6. HRMS m/z calculated for $C_{60}H_{71}N_{12}O_8S_2$ $[M + H]^+$: 1151.4954; found: 1151.4931.

Compound 4. FTIR (neat): 3150.13, 3100.92, 2950.45, 2834.56, 1651.92, 1635.04, 1553.55, 1539.09, 1516.91, 1435.90, 1419.03, 1199.16, 1173.60, 1127.80, 1021.24, 951.81 cm^{-1}. ^1H NMR (400 MHz, CD_3OD): δ 8.48−8.3 (m 1H), 8.38 (d, 1H, J = 4.89), 7.75−7.67 (m, 2H), 7.66 (d, 1H, J = 7.83), 7.38 (dd, 2H, J = 4.40, J = 4.40), 7.35−7.15 (m, 12H), 7.05 (dd, 2H, J = 1.96, J = 1.46), 5.22−5.16 (m, 2H), 4.91 (d, 1H, J = 3.91), 4.81 (d, 1H, J = 3.91), 4.42 (q, 2H, J = 6.84, J = 1.95, J = 6.35), 4.34 (q, 2H, J = 4.89, J = 3.42, J = 4.89), 3.94 (m, 2H), 3.75 (m, 2H), 3.62 (d, 1H, J = 2.44), 3.26−3.17 (m, 4H), 2.86−2.75 (m, 4H), 2.64 (s, 3H). ^{13}C NMR (100 MHz, CD_3OD): δ 18.59, 24.45, 24.38, 27.05, 28.78, 35.45, 36.64, 38.98, 50.57, 55.11, 60.89, 125.86, 126.51, 128.16, 128.82, 134.63, 136.96, 140.43, 145.59, 147.31, 166.74, 170.23, 172.50. HRMS m/z calculated for $C_{54}H_{71}N_{12}O_8S_2$ $[M + H]^+$: 1079.4954; found: 1079.4957

Compound 5. FTIR (neat): 3068.39, 3029.00, 2995.31, 2967.15, 2950.40, 2932.08, 2929.67, 1655.29, 1650.95, 1645.171575.25, 1524.14, 1488.46, 1444.10, 1435.42, 1388.17, 1350.08, 1320.18, 1199.64, 1176.50, 1131.65, 1001.95, 959.05 cm^{-1}. ^1H NMR (400 MHz, CD_3OD): δ 7.35−7.27 (m, 10H), 4.64−4.49 (tt, 6H, J = 3.66, J = 5.79, J = 5.49, J = 6.71), 3.86−3.80, (m, 2H), 3.79−3.70 (m, 2H, 3.55−3.49 (tt, J = 4.57, J = 7.62, J = 5.19, J = 5.79, J = 8.55) 3.28−3.09 (m, 10H), 2.90−2.71 (m, 6H), 2.29−2.24 (m, 2H), 2.14−2.06 (m, 7H), 1.99−1.73 (m, 5H). ^{13}C NMR (125 MHz, CD_3OD): δ 173.33, 172.97, 166.88, 162.37, 137.67, 129.94, 129.10, 129.03, 127.48, 61.31, 56.19, 51.57, 49.00, 48.83, 48.66, 48.49, 48.32, 48.15, 47.98, 39.91, 38.19, 37.79, 37.49, 36.37, 29.92, 27.99, 25.60. HRMS m/z calculated for $C_{40}H_{61}N_{10}O_6S_2$ $[M + H]^+$: 841.4211; found: 841.4208.

Compound 6. FTIR (neat): 3021.78, 2985.12, 2966.80, 2920.51, 1668.31, 1651.92, 1634.56, 1538.61, 1468.69, 1464.35, 1298.00, 1265.70, 1231.46, 1198.88, 1173.60, 1050.34 cm^{-1}. ^1H NMR (400 MHz, CD_3OD): δ 8.46 (d, 1H, J = 16.62), 8.37 (s, 2H), 7.29−7.20 (m, 18H), 7.06 (d, 6H, J = 7.83), 6.22 (d, 4H, J = 4.40), 5.54 (s, 2H), 5.28 (q, 1H, J = 4.48, J = 4.40, J = 4.48), 4.44, (m, 2H), 3.89 (q, 1H, J = 7.34, J = 6.85), 3.89 (q, 1H, J = 7.34, J = 6.85), 3.79 (q, 3H, J = 8.80, J = 6.35), 3.43 (dd, 1H,

J = 8.91, J = 8.91), 3.29−2.95 (m, 10H), 2.74 (q, 2H, J = 6.85, J = 6.85), 2.68, (d, 1H, J = 1.96), 2.64 (q, 2H), 2.06 (m, 2H), 1.94 (q, 2H, J = 6.35, J = 6.84, J = 8.31), 1.72 (t, 3H, J = 6.84), 1.27 (t, 3H, J = 7.82). ^{13}C NMR (100 MHz, CD_3OD): δ 172.5, 171.12, 169.52, 167.55, 157.77, 149.46, 143.96, 136.89, 128.89, 129.02, 125.86, 103.39,102.95, 60.59, 56.63, 55.142, 38.99, 36.61, 35.466, 28.92, 27.05, 24.51, 13.45. HRMS m/z calculated for $C_{66}H_{79}N_{12}O_{12}S_2$ $[M + H]^+$: 1295.5376; found: 1295.5350.

Compound 7. FTIR (neat): 3100.23, 3050.10, 2950.66, 1690.89, 168.31, 1668.28, 1652.40, 1635.04, 1567.89, 1234.99, 1200.61, 1174.09, 1129.24 cm^{-1}. ^{1}H NMR (400 MHz, CD_3OD): δ 8.64 (d, 2H, J = 1.96), 8.33−8.18 (m, 9H), 7.85 (m, 4H), 7.32−5.15 (m, 14H), 5.16 (q, 2H, J = 6.36, J = 2.44, J = 5.87), 4.46 (m, 4H), 3.95 (q, 2H, J = 9.78, J = 7.34, J = 6.85), 3.78 (m 2H), 3.27 (m, 4H), 3.24 (d, 4H), 3.20−3.08 (m, 6H), 3.04−2.95 (m, 4H), 2.7 (m, 5H), 2.6 (d, 4H, J = 4.40), 2.15 (m, 2H), 2.01−1.85 (m, 2H), 1.69 (t, 4H, J = 6.84), 1.29 (d, 4H, J = 3.913). ^{13}C NMR (100 MHz, CD_3OD): δ 182.07, 182.02, 172.53, 170.42, 166.74, 138.36, 136.89, 135.20, 134.19, 133,40, 133.23, 132.50, 128.80, 128.72, 28.16, 127.02, 126.70, 126.54, 125.81, 60.84, 55.09, 51.96, 40.41, 38.98, 36.83, 36.61, 35.45, 28.89, 28.76, 27.07, 24.44. HRMS m/z calculated for $C_{70}H_{73}N_{10}O_{12}S_2$ $[M + H]^+$: 1309.4845; found: 1309.4823.

Synthesis of Dicarba Analogues. Resin-bound **8** was synthesized using standard Fmoc methodology for peptide synthesis. Wang resin (1.0 g, 100−200 mesh, 1 mmol/g loading) was activated with 1,1′-carbonyldiimidazole (DIC, 3.3 g, 10 mmol) in 12 mL of DMF for 12 h on a LabQuake rotator. The resin was then washed three times each with DMF, CH_2Cl_2, and DMF again, followed by reaction with 1,3-diaminopropane (0.72 mL, 10 mmol) in DMF (12 mL) for another 12 h. The wash cycle was then repeated. The coupling of the first amino acid was carried out by adding Fmoc-L-Phe-OH (1.16 g, 3 mmol), HBTU (1.14 g, 3 mmol), and DIPEA (0.85 mL, 5 mmol) in 12 mL of DMF to the resin and rotating the reaction mixture for 1 h. Following a wash cycle, Fmoc deprotection was accomplished using 20% piperidine in CH_2Cl_2 for 0.5 h followed again by the wash cycle. Similarly, Fmoc-L-Pro-OH, Fmoc-L-allylglycine, and 2-ethylquinoline-3-carboxylic acid were coupled to synthesize resin-bound monomeric compound (**8**).

The resin was then split into two equal parts of 0.50 g. One part was treated with 30% TFA/1% TEA in CH_2Cl_2 for 0.5 h to obtain a cleaved product **8** (0.23 g) to be used as the solution olefin component for the metathesis reaction. The other part of the resin was dried in a desiccator under vacuum for 12 h and then allowed to swell in dry CH_2Cl_2 (12 mL) for 20 min. The resin was washed with CH_2Cl_2 (3 × 10 mL) followed by 0.8 M LiCl in DMF (10 mL) for 10 min. The resin was then washed with DMF (10 mL), and the 0.8 M LiCl wash was repeated for two more times. Finally, the resin was washed with dry, degassed 1,2-dichloroethane (10 mL) and then suspended in the same solvent (5 mL). To this suspension were added Grubbs' second generation catalyst (0.14 g, 0.17 mmol) in 5 mL of 1,2-dichloroethane and the cleaved **8** (0.25 g, 0.42 mmol) in 10 mL of a 1:4 mixture of CH_2Cl_2 and 1,2-dichloroethane. The reaction mixture was refluxed for 24 h. The reaction was then cooled to room temperature, and additional Grubbs' second generation catalyst (0.07 g, 0.09 mmol) was added to the reaction mixture and refluxed for another 24 h. After repeating this cycle a third time, the reaction mixture was cooled to room temperature and transferred to a standard solid-phase reaction vessel with filtering. The resin was then washed with CH_2Cl_2 (3 × 10) and DMF (3 × 10 mL) and suspended in 10 mL of DMF. DMSO (0.2 mL) was added to the suspension and rotated for 12 h, in order to remove colored ruthenium impurities.[46] The resin was then washed and the product cleaved off the resin with 25% TFA in CH_2Cl_2 (10 mL) for 0.5 h to obtain a crude mixture of olefins **9** and **10** (0.25 g, 64%). The isomers were then separated using preparative RP-HPLC (isocratic elution, 30% acetonitrile in water with 0.1% TFA).

Compound 8. FTIR (neat): 3249, 2934, 2817, 1672, 1659, 1643, 1634, 1529, 1517, 1201, 1177, 1128, 1026 cm^{-1}. ^{1}H NMR (400 MHz, $CDCl_3$): δ 8.90 (s, 1H), 8.30 (t, 1H, J = 8.8), 8.09 (d, 1H, J = 8.4), 8.03 (t, 1H, J = 7.8), 7.82 (t, 1H, J = 7.8), 7.71−7.69 (m, 3H), 7.31−7.27 (m, 3H), 7.12 (d, 2H, J = 6.8), 5.88−5.84 (m, 1H), 5.34−5.24 (m, 2H), 4.49−4.88 (m, 1H), 4.59−4.5 (m, 1H), 4.32−4.28 (m, 1H), 3.98 (s, 1H), 3.68−3.62 (m, 1H), 3.39−3.21 (m, 4H), 3.11−3.10 (m, 2H), 2.94−2.90 (m, 2H), 2.46−2.42 (m, 2H), 2.22−2.13 (m, 1H), 2.07−2.01 (m, 1H), 1.96−1.90 (m, 1H), 1.85−1.80 (m, 3H), 1.35 (t, 3H, J = 7.4), 1.25 (s, 2H). ^{13}C NMR (100 MHz, $CDCl_3$): 172.2, 171.9, 171.4, 166.2, 161.4, 136.4, 132.6, 129.7, 129.0, 128.6, 128.4, 127.1, 126.1, 119.3, 61.4, 54.5, 51.4, 47.9, 37.0, 36.7, 35.9, 35.8, 28.7, 27.4, 26.8, 24.9, 15.2, 14.2. HRMS m/z calculated for $C_{34}H_{42}N_6O_4$ $[M + H]^+$: 599.3346; found: 599.3357.

Compound 9. FTIR (neat): 2957.1, 2920.2, 2853.5, 1673.1, 1667.8, 1457.1, 1377.0, 1201.1, 1179.3, 1134.1 cm^{-1}. ^{1}H NMR (500 MHz, CD_3OD): δ 8.63 (s, 2H), 8.08 (d, 2H, J = 8.0), 8.04 (d, 2H, J = 9.0), 7.89 (t, 2H, J = 8), 7.68 (t, 2H, J = 8.0), 7.21−7.11 (m, 10H), 5.78 (m, 2H), 4.48−4.42 (m, 2H), 4.36 (t, 2H, J = 7.5), 3.92−3.88 (m, 2H), 3.66−3.60 (m, 4H), 3.55−3.51 (m, 1H), 3.17−3.10 (m, 4H), 3.02−2.90 (m, 4H), 2.81 (s, 1H), 2.17−2.62 (m, 6H), 2.54−2.52 (m, 1H), 2.15−2.08 (m, 2H), 1.91−1.88 (m, 4H), 1.83−1.79 (m, 2H), 1.68−1.63 (m, 5H), 1.34−1.21 (m, 8H), 0.87−0.80 (m, 2H). ^{13}C NMR (100 MHz, CD_3OD): 173.9, 171.9, 168.8, 162.3, 138.0, 134.2, 130.7, 130.2, 130.1, 129.9, 129.8, 129.5, 129.4, 129.3, 127.8, 127.4, 61.5, 56.5, 53.3, 38.4, 37.9, 36.7, 35.0, 29.1, 28.4, 25.9, 14.5. HRMS m/z calculated for $C_{66}H_{80}N_{12}O_8$ $[M + H]^+$: 1169.6300; found: 1169.6296

Compound 10. FTIR (neat): 2957.6, 2920.0, 2900.7, 2851.1, 1664.3, 1634.3, 1557.4, 1538.6, 1201.1, 1180.3, 1133.1 cm^{-1}. ^{1}H NMR (500 MHz, CD_3OD): δ 8.67 (s, 2H), 8.11−8.05 (m, 4H), 7.98−7.93 (m, 2H), 7.77−7.71 (m, 2H), 7.25−7.17 (m, 10H), 5.82−5.79 (m, 2H), 4.97−4.94 (m, 1H), 4.48−4.45 (m, 2H), 3.97−3.92 (m, 2H), 3.72−3.65 (m, 4H), 3.21−3.16 (m, 8H), 3.05−3.20 (m, 4H), 2.76−2.69 (m, 6H), 2.18−2.12 (m, 2H), 1.97−1.93 (m, 3H), 1.87−1.83 (m, 2H), 1.72−1.69 (m, 4H), 1.39−1.28 (m, 10H). ^{13}C NMR (100 MHz, CD_3OD): δ 172.6, 172.5, 170.3, 167.7, 161.0, 136.8, 132.8, 129.5, 128.7, 128.5, 128.1, 127.9, 127.6, 126.5, 126.1, 124.2, 69.8, 60.3, 55.2, 51.9, 37.1, 36.6, 35.4, 29.0, 27.6, 24.6, 13.2. HRMS m/z calculated for $C_{66}H_{80}N_{12}O_8$ $[M + H]^+$: 1169.6300; found: 1169.6297

Compound 11. Hydrogenation was performed on resin. The resin-bound olefin metathesis product (resin: 0.25 g, 0.25 mmol) was suspended in 6 mL of 10% MeOH in CH_2Cl_2 in a 16 mL glass vial. Wilkinson's catalyst (0.06 g, 0.06 mmol) was added to this suspension, and the mixture was agitated on a Parr hydrogenator under 40 psi H_2 gas pressure at room temperature for 5 h. The resin was then washed with 10% MeOH in CH_2Cl_2 (3 × 10 mL), MeOH (3 × 10 mL), and CH_2Cl_2 (3 × 10 mL). The resin-bound reduced product was then cleaved using 30% TFA/1% TES in CH_2Cl_2 (6 mL). The cleaved product was collected, and the solvent was removed *in vacuo*. The crude product was then precipitated using cold ether and centrifuged (5000*g*, 5 min), and the ether was decanted to obtain pure **11** in 60% yield (0.08 g).

FTIR (neat): 3300.3, 2959.5, 2910.2, 1675.4, 1652.4, 1641.2, 1621.5, 1535.7, 1199.2, 1190.5, 1177.0, 1124.9 cm^{-1}. ^{1}H NMR (500 MHz, CD_3OD): δ 8.67 (s, 2H), 8.10−8.05 (m, 4H), 7.95−7.91 (m, 2H), 7.74−7.69 (m, 2H), 7.24−7.20 (m, 10H), 4.50−4.40 (m, 4H), 4.20 (dd, 2H, J_1 = 7.5, J_2 = 2.5), 4.03−3.98 (m, 2H), 3.82−3.64 (m, 3H), 3.48 (q, 2H, J = 17.5), 3.27−3.14 (m, 10H), 3.05−3.02 (m, 4H), 2.98 (br s, 2H), 2.78−2.67 (m, 4H), 2.22−2.09 (m, 3H), 1.73−1.65 (m, 4H), 1.39−1.28 (m, 6H), 0.99−0.89 (m, 4H), 0.59 (m, 2H). ^{13}C NMR (100 MHz, CD_3OD): δ 172.6, 172.5, 161.2, 161.0, 138.3, 136.8, 131.9, 129.6, 128.9, 128.1, 127.3, 126.4, 125.9, 125.3, 60.2, 55.2, 51.8, 36.9, 36.5, 35.3, 28.9, 28.3, 27.0, 25.1, 24.6, 13.2. HRMS m/z

calculated for $C_{66}H_{82}N_{12}O_8Na$ $[M + Na]^+$: 1193.6271; found: 1193.6243

Cell Culture and *in Vitro* Cytotoxicity Assay. Human fibroblast cells were cultured in Dulbecco's modified Eagle's medium (DMEM), containing 5% fetal bovine serum (Invitrogen) and 5% pen-strep. Cell cultures were incubated in a humidified atmosphere containing 5% CO_2 at 37 °C. The viability of human fibroblasts in the presence of compound **10** was tested using the 3-(4,5-dimethylthiazol-2-yl)-2,5-diphenyltetrazolium bromide (MTT) assay. Cells were plated in a 96-well sterile plate at concentrations of 3.2×10^4 cells per well in a volume of 100 μL of culture media. The cells were then allowed to grow to approximately 80% confluence by incubating at 37 °C for 48 h. The old media were removed and replaced with 100 μL of different concentrations (up to 1 mM) of compound **10** or mitomycin C (as a control) in DMEM. Cells were exposed to compounds for period of 24 h, after which the media were removed. Next, MTT was added to each of the wells and incubated for 4 h. Isopropyl alcohol was added to the cells after removal of the MTT medium followed by absorbance measurement at 600 nm. Absorbance values were obtained on a Modulus microplate reader (Turner Biosystems).

Acknowledgment. The authors gratefully acknowledge financial support of the NIH/NIAID P30AI078498, via the University of Rochester Developmental Center for AIDS Research (DCFAR), and NIH T32AR007472 (training grant support to P.C.G.). We thank Prof. Thomas Foster for the use of his fluorometer and Prof. Lisa DeLouise for guidance with the MTT assays.

Supporting Information Available: Spectral data for compounds **2**−**11**, selected fluorescence titration data for compounds **2**−**11**, SPR data and controls for compounds **9** −**11**, and dynamic light scattering data for compounds **9** −**11**. This material is available free of charge via the Internet at http://pubs.acs.org.

References

(1) For reviews, see: (a) Tor, Y. Targeting RNA with small molecules. *ChemBioChem* **2003**, *4*, 998–1007. (b) Thomas, J. R.; Hergenrother, P. J. Targeting RNA with small molecules. *Chem. Rev.* **2008**, *108*, 1171–1224.

(2) Dervan, P. B.; Bürli, R. W. Sequence-specific DNA recognition by polyamides. *Curr. Opin. Chem. Biol.* **1999**, *3*, 688–693.

(3) Wender, P. A.; Miller, B. L. Synthesis at the molecular frontier. *Nature* **2009**, *460*, 197–201.

(4) Flexner, C. HIV drug development: the next 25 years. *Nat. Rev. Drug Discovery* **2007**, *6*, 959–966.

(5) Martinez-Cajas, J. L.; Wainberg, M. A. Protease inhibitor resistance in HIV-infected patients: molecular and clinical perspectives. *Antiviral Res.* **2007**, *76*, 203–221.

(6) De Clercq, E. HIV resistance to reverse transcriptase inhibitors. *Biochem. Pharmacol.* **1994**, *47*, 155–169.

(7) Struble, K.; Murray, J.; Cheng, B.; Gegeny, T.; Miller, V.; Gulick, R. Antiretroviral therapies for treatment-experienced patients: current status and research challenges. *AIDS* **2005**, *19*, 747–756.

(8) (a) Zapp, M. L.; Stern, S.; Green, M. R. Small molecules that selectively block RNA binding of HIV-1 Rev protein inhibit Rev function and viral production. *Cell* **1993**, *74*, 969–978. (b) Battiste, J. L.; Mao, H.; Rao, N. S.; Tan, R.; Muhandiram, D. R.; Kay, L. E.; Frankel, A. D.; Williamson, J. R. Alpha helix-RNA major groove recognition in an HIV-1 rev peptide-RRE RNA complex. *Science* **1996**, *273*, 1547–1551. (c) Kirk, S. R.; Luedtke, N. W.; Tor, Y. Neomycin-acridine conjugate: a potent inhibitor of Rev-RRE binding. *J. Am. Chem. Soc.* **2000**, *122*, 980–981. (d) Hendrix, M.; Priestley, E. S.; Joyce, G. F.; Wong, C. H. Direct observation of aminoglycoside-RNA interactions by surface plasmon resonance. *J. Am. Chem. Soc.* **1997**, *119*, 3641–3648.

(9) Mei, H. Y.; Cui, M.; Heldsinger, A.; Lemrow, S. M.; Loo, J. A.; Sannes-Lowery, K. A.; Sharmeen, L.; Czarnik, A. W. Inhibitors of protein-RNA complexation that target the RNA: specific recognition of human immunodeficiency virus type 1 TAR RNA by small organic molecules. *Biochemistry* **1998**, *37*, 14204–14212.

(10) (a) Tang, H.; Kuhen, K. L.; Wong-Staal, F. Lentivirus replication and regulation. *Annu. Rev. Genet.* **1999**, *33*, 133–170. (b) Frankel, A. D.; Young, J. A. HIV-1: fifteen proteins and an RNA. *Annu. Rev. Biochem.* **1998**, *67*, 1–25. (c) Ludwig, V.; Krebs, A.; Stoll, M.; Dietrich, U.; Ferner, J.; Schwalbe, H.; Scheffer, U.; Dürner, G.; Göbel, M. W. Tripeptides from synthetic amino acids block the Tat-TAR association and slow down HIV spread in cell cultures. *ChemBioChem* **2007**, *8*, 1850–1856. (d) Wang, D.; Iera, J.; Baker, H.; Hogan, P.; Ptak, R.; Yang, L.; Hartman, T.; Buckheit, R. W., Jr.; Desjardins, A.; Yang, A.; Legault, P.; Yedavalli, V.; Jeang, K.-T.; Appella, D. H. Multivalent binding oligomers inhibit HIV Tat-TAR interaction critical for viral replication. *Bioorg. Med. Chem. Lett.* **2009**, *19*, 6893–6897.

(11) (a) Jacks, T.; Power, M. D.; Masiarz, F. R.; Luciw, P. A.; Barr, P. J.; Varmus, H. E. Characterization of ribosomal frameshifting in HIV-1 gag-pol expression. *Nature* **1988**, *331*, 280–283. (b) Parkin, N. T.; Chamorro, M; Varmus, H. E. Human immunodeficiency virus type 1 gag-pol frameshifting is dependent on downstream mRNA secondary structure: demonstration by expression in vivo. *J. Virol.* **1992**, *66*, 5147–5151.

(12) (a) Park, J.; Morrow, C. D. Overexpression of the gag-pol precursor from human immunodeficiency virus type 1 proviral genomes results in efficient proteolytic processing in the absence of virion production. *J. Virol.* **1991**, *65*, 5111–5117. (b) Karacostas, V.; Wolffe, E. J.; Nagashima, K.; Gonda, M. A.; Moss, B. Overexpression of the HIV-1 gag-pol polyprotein results in intracellular activation of HIV-1 protease and inhibition of assembly and budding of virus-like particles. *Virology* **1993**, *193*, 661–671. (c) Hung, M.; Patel, P.; Davis, S.; Green, S. R. Importance of ribosomal frameshifting for human immunodeficiency virus type 1 particle assembly and replication. *J. Virol.* **1998**, *72*, 4819–4824. (d) Shehu-Xhilaga, M.; Crowe, S. M.; Mak, J. Maintenance of the Gag/Gag-Pol ratio is important for human immunodeficiency virus type 1 RNA dimerization and viral infectivity. *J. Virol.* **2001**, *75*, 1834–1841. (e) Dulude, D.; Berchiche, Y. A.; Gendron, K.; Brakier-Gingras, L.; Heveker, N. Decreasing the frameshift efficiency translates into an equivalent reduction of the replication of the human immunodeficiency virus type 1. *Virology* **2006**, *345*, 127–136.

(13) (a) Dulude, D.; Baril, M.; Brakier-Gingras, L. Characterization of the frameshift stimulatory signal controlling a programmed −1 ribosomal frameshift in the human immunodeficiency virus type 1. *Nucleic Acids Res.* **2002**, *30*, 5094–5102.

(14) (a) Telenti, A.; Martinez, R.; Munoz, M.; Bleiber, G.; Greub, G.; Sanglard, D.; Peters, S. Analysis of natural variants of the human immunodeficiency virus type 1 gag-pol frameshift stem-loop structure. *J. Virol.* **2002**, *76*, 7868–7873. (b) Baril, M.; Dulude, D.; Gendron, K.; Lemay, G.; Brakier-Gingras, L. Efficiency of a programmed −1 ribosomal frameshift in the different subtypes of the human immunodeficiency virus type 1 group M. *RNA* **2003**, *9*, 1246–1253.

(15) Hung, M.; Patel, P.; Davis, S.; Green, S. R. Importance of ribosomal frameshifting for human immunodeficiency virus type 1 particle assembly and replication. *J. Virol.* **1998**, *72*, 4819–4824.

(16) Gareiss, P. C.; Miller, B. L. Ribosomal frameshifting: an emerging target in HIV. *Curr. Opin. Invest. Drugs* **2009**, *10*, 121–128.

(17) (a) Staple, D. W.; Butcher, S. E. Solution structure of the HIV-1 frameshift inducing stem-loop RNA. *Nucleic Acids Res.* **2003**, *31*, 4326–4331. (b) Staple, D. W.; Butcher, S. E. Solution structure and thermodynamic investigation of the HIV-1 frameshift inducing element. *J. Mol. Biol.* **2005**, *349*, 1011. (c) Gaudin, C.; Mazauric, M. H.; Traikia, M.; Guittet, E.; Yoshizawa, S.; Fourmy, D. Structure of the RNA signal essential for translational frameshifting in HIV-1. *J. Mol. Biol.* **2005**, *349*, 1024–1035.

(18) (a) Green, L.; Kim, C.-H.; Bustamante, C.; Tinoco, I. Characterization of the mechanical unfolding of RNA pseudoknots. *J. Mol. Biol.* **2008**, *375*, 511–528. (b) Chen, G.; Chang, K.; Chou, M.; Bustamante, C.; Tinoco, I. Triplex structures in an RNA pseudoknot enhance mechanical stability and increase efficiency of −1 ribosomal frameshifting. *Proc. Natl. Acad. Sci. U.S.A.* **2009**, *106*, 12706–12711.

(19) Mazauric, M.-H.; Seol, Y.; Yoshizawa, S.; Visscher, K.; Fourmy, D. Interaction of the HIV-1 frameshift signal with the ribosome. *Nucleic Acids Res.* **2009**, *37*, 7654–7664.

(20) McNaughton, B. R.; Gareiss, P. C.; Miller, B. L. Identification of a selective small-molecule ligand for HIV-1 frameshift-inducing stem-loop RNA from an 11,325 member resin bound dynamic combinatorial library. *J. Am. Chem. Soc.* **2007**, *129*, 11306–11307.

(21) (a) Addess, K. J.; Sinsheimer, J. S.; Feigon, J. Solution structure of a complex between [N-MeCys3,N-MeCys7]TANDEM and [d(GATATC)]2. *Biochemistry* **1993**, *32*, 2498–2508. (b) Addess, K. J.; Feigon, J. Sequence specificity of quinoxaline antibiotics. 1. Solution structure of a 1:1 complex between triostin A and [d(GACGTC)]2 and

comparison with the solution structure of the [N-MeCys3,N-MeCys7]-TANDEM-[d(GATATC)]2 complex. *Biochemistry* **1994**, *33*, 12386–12397.
(22) Staple, D.; Venditti, V.; Niccolai, N.; Elson-Schwab, L.; Tor, Y.; Butcher, S. Guanidinoneomycin B recognition of an HIV-1 RNA helix. *ChemBioChem* **2007**, *9*, 93–102.
(23) Marcheschi, R. J.; Mouzakis, K. D.; Butcher, S. E. Selection and characterization of small molecules that bind the HIV-1 frameshift site RNA. *ACS Chem. Biol.* **2009**, *4*, 844–854.
(24) Dulude, D.; Théberge-Julien, G.; Brakier-Gringras, L.; Heveker, N. Selection of peptides interfering with a ribosomal frameshift in the human immunodeficiency virus type 1. *RNA* **2008**, *14*, 981–991.
(25) (a) McCutchan, F. E. Understanding the genetic diversity of HIV-1. *AIDS* **2000**, *14*, S31–S44. (b) Robertson, D. L.; Anderson, J. P.; Bradac, J. A.; Carr, J. K.; Foley, B.; Funkhouser, R. K.; Gao, F.; Hahn, B. H.; Kalish, M. L.; Kuiken, C.; Learn, G. H.; Leitner, T.; McCutchan, F.; Somanov, S.; Peeters, M.; Pieniazek, D.; Salminen, B.; Sharp, P. M.; Wolinsky, S.; Korber, B. HIV-1 nomenclature proposal. *Science* **2000**, *288*, 55–56.
(26) Liu, X.; Thomas, J. R.; Hergenrother, P. J. Deoxystreptamine dimers bind to RNA hairpin loops. *J. Am. Chem. Soc.* **2004**, *126*, 9196–9197.
(27) Llano-Sotelo, B.; Chow, C. S. RNA-aminoglycoside antibiotic interactions: Fluorescence detection of binding and conformational change. *Bioorg. Med. Chem. Lett.* **1999**, *9*, 213–216.
(28) Luedtke, N. W.; Liu, Q.; Tor, Y. RNA-ligand interactions: affinity and specificity of aminoglycoside dimers and acridine conjugates to the HIV-1 Rev response element. *Biochemistry* **2003**, *42*, 11391–11403.
(29) (a) Sequence 10: Karan, C.; Miller, B. L. RNA-selective coordination complexes identified via dynamic combinatorial chemistry. *J. Am. Chem. Soc.* **2001**, *123*, 7455–7456. (b) Sequence 11: Gareiss, P. C.; Sobczak, K.; McNaughton, B. R.; Palde, P. B.; Thornton, C. A.; Miller, B. L. Dynamic combinatorial selection of small molecules capable of inhibiting the (CUG) repeat RNA−MBNL1 interaction in vitro: discovery of lead compounds targeting myotonic dystrophy (DM1). *J. Am. Chem. Soc.* **2008**, *130*, 16254–16261.
(30) Szajewski, R. P.; Whitesides, G. M. Rate constants and equilibrium constants for thiol-disulfide interchange reactions involving oxidized glutathione. *J. Am. Chem. Soc.* **1980**, *102*, 2011–2026.
(31) Hwang, C.; Sinskey, A. J.; Lodish, H. F. Oxidized redox state of glutathione in the endoplasmic reticulum. *Science* **1992**, *257*, 1496–1502.
(32) (a) Fotouhi, N.; Joshi, P.; Tilley, J. W.; Rowan, K.; Schwinge, V.; Wolitzky, B. Cyclic thioether peptide mimetics as VCAM-VLA-4 antagonists. *Bioorg. Med. Chem. Lett.* **2000**, *10*, 1167–1169. (b) Stymiest, J. L.; Mitchell, B. F.; Wong, S.; Vederas, J. C. Synthesis of biologically active dicarba analogues of the peptide hormone oxytocin using ring-closing metathesis. *Org. Lett.* **2003**, *5*, 47–49. (c) Berezowska, I.; Chung, N. N.; Lemieux, C.; Wilkes, B. C.; Schiller, P. W. Dicarba analogues of the cyclic enkephalin peptides H-Tyr-c[D-Cys-Gly-Phe-D(or L)-Cys]NH(2) retain high opioid activity. *J. Med. Chem.* **2007**, *50*, 1414–1417. (d) Mollica, A.; Guardiani, G.; Davis, P.; Ma, S.; Porreca, F.; Lai, J.; Mannina, L.; Sobolev, A. P.; Hruby, V. J. Synthesis of stable and potent delta/mu opioid peptides: analogues of H-Tyr-c[D-Cys-Gly-Phe-D-Cys]-OH by ring-closing metathesis. *J. Med. Chem.* **2007**, *50*, 3138–3142.
(33) Nicolaou, K. C.; Hughes, R.; Cho, S. Y.; Winssinger, N.; Smethurst, C.; Labischinski, H.; Endermann, R. Target-accelerated combinatorial synthesis and discovery of highly potent antibiotics effective against vancomycin-resistant bacteria. *Angew. Chem., Int. Ed.* **2000**, *39*, 3823–3828.
(34) Hoveyda, A. H.; Zhugralin, A. R. The remarkable metal-catalysed olefin metathesis reaction. *Nature* **2007**, *250*, 243–251.
(35) (a) Wels, B.; Kruijtzer, J. A.; Garner, K.; Nijenhuis, W. A.; Gispen, W. H.; Adan, R. A.; Liskamp, R. M. Synthesis of a novel potent cyclic peptide MC4-ligand by ring-closing metathesis. *Bioorg. Med. Chem.* **2005**, *13*, 4221–4227. (b) Stymiest, J. L.; Mitchell, B. F.; Wong, S.; Vederas, J. C. Synthesis of oxytocin analogues with replacement of sulfur by carbon gives potent antagonists with increased stability. *J. Org. Chem.* **2005**, *70*, 7799–7809.
(36) McNaughton, B. R.; Bucholtz, K. M.; Camaano-Moure, A.; Miller, B. L. Self-selection in olefin cross metathesis: the effect of remote functionality. *Org. Lett.* **2005**, *7*, 733–736.
(37) (a) Myers, A. G.; Schnider, P.; Kwon, S.; Kung, D. W. Greatly simplified procedures for the synthesis of alpha-amino acids by the direct alkylation of pseudoephedrine glycinamide hydrate. *J. Org. Chem.* **1999**, *64*, 3322–3327. (b) Ryan, S. J.; Zhang, Y.; Kennan, A. J. Convenient access to glutamic acid side chain homologues compatible with solid phase peptide synthesis. *Org. Lett.* **2005**, *7*, 4765–4767.
(38) Galan, B. R.; Kalbarczyk, K. P.; Szczepankiewicz, S.; Keister, J. B.; Diver, S. T. A rapid and simple cleanup procedure for metathesis reactions. *Org. Lett.* **2007**, *9*, 1203–1206.
(39) Swinney, D. C. Biochemical mechanisms of drug action: what does it take for success? *Nat. Rev. Drug Discovery* **2004**, *3*, 801–808.
(40) Copeland, R. A.; Pompliano, D. L.; Meek, T. D. Drug-target residence time and its implications for lead optimization. *Nat. Rev. Drug Discovery* **2006**, *5*, 730–739.
(41) Dierynck, I.; De Wit, M.; Gustin, E.; Keuleers, I.; Vandersmissen, J.; Hallenberger, S.; Hertogs, K. Binding kinetics of darunavir to human immunodeficiency virus type 1 protease explain the potent antiviral activity and high genetic barrier. *J. Virol.* **2007**, *81*, 13845–13851.
(42) Hendrix, M.; Priestley, E. S.; Joyce, G. F.; Wong, C. H. Direct observation of aminoglycoside-RNA interactions by surface plasmon resonance. *J. Am. Chem. Soc.* **1997**, *119*, 3641–3648.
(43) Begg, E. J.; Barclay, M. L. Aminoglycosides—50 years on. *Br. J. Clin. Pharmacol.* **1995**, *39*, 597–603.
(44) Mosmann, T. Rapid colorimetric assay for cellular growth and survival: application to proliferation and cytotoxicity assays. *J. Immunol. Methods* **1983**, *65*, 55–63.
(45) (a) Motulsky, H.; Christopoulos, A. Analyzing saturation binding with ligand depletion. In *Fitting Models to Biological Data Using Linear and Nonlinear Regression. A Practical Guide to Curve Fitting*, Oxford University Press: New York, 2004; pp 208−210; (b) *Fluorescence Polarization Technical Resource Guide*, Invitrogen, Inc., 2006; Chapter 7.
(46) Ahn, Y. M.; Yang, K.; Georg, G. I. A convenient method for the efficient removal of ruthenium byproducts generated during olefin metathesis reactions. *Org. Lett.* **2001**, *3*, 1411–1413.